

PCCP

Accepted Manuscript



This is an *Accepted Manuscript*, which has been through the Royal Society of Chemistry peer review process and has been accepted for publication.

Accepted Manuscripts are published online shortly after acceptance, before technical editing, formatting and proof reading. Using this free service, authors can make their results available to the community, in citable form, before we publish the edited article. We will replace this *Accepted Manuscript* with the edited and formatted *Advance Article* as soon as it is available.

You can find more information about *Accepted Manuscripts* in the [Information for Authors](#).

Please note that technical editing may introduce minor changes to the text and/or graphics, which may alter content. The journal's standard [Terms & Conditions](#) and the [Ethical guidelines](#) still apply. In no event shall the Royal Society of Chemistry be held responsible for any errors or omissions in this *Accepted Manuscript* or any consequences arising from the use of any information it contains.

**On the Characterization of NaDEHP/*n*-Heptane Nonaqueous Reverse Micelles.
Effect of the Polar Solvent.**

Dra. Silvina S. Quintana, Dr. R. Dario Falcone, Prof. Juana J. Silber, Dr. Fernando
Moyano*, Prof. N. Mariano Correa*.

*Departamento de Química. Universidad Nacional de Río Cuarto. Agencia Postal # 3.
C.P. X5804BYA Río Cuarto. ARGENTINA*

[*] Dr. N. Mariano Correa, Dr. Fernando Moyano. Corresponding-Author,
Departamento de Química. Universidad Nacional de Río Cuarto. Agencia Postal # 3.
C.P. X5804BYA Río Cuarto. ARGENTINA. E-mail: mcorrea@exa.unrc.edu.ar,
fmoyano@exa.unrc.edu.ar

Dra. Silvina S. Quintana, Dr. R. Dario Falcone, Prof. Juana J. Silber,
Departamento de Química. Universidad Nacional de Río Cuarto. Agencia Postal # 3.
C.P. X5804BYA Río Cuarto. ARGENTINA.

KEYWORDS

NaDEHP; Non-Aqueous Reverse Micelles; Microenvironment; Micropolarity; QB; FT-IR

ABSTRACT

The behavior of two polar solvents, ethylene glycol (EG) and dimethylformamide (DMF), entrapped in *n*-heptane/sodium bis-(2-ethylhexyl) phosphate (NaDEHP) reverse micelles (RMs) were investigated using dynamic light scattering (DLS), molecular probe absorption and FT-IR spectroscopy. DLS results reveal the formation of RMs containing EG and DMF as a polar component. To the best of our knowledge this is the first report where both polar solvents are entrapped by NaDEHP surfactant to effectively create RMs.

We use the solvatochromism behavior of the molecular probe, 1-methyl-8-oxyquinolinium betaine (QB) and FT-IR spectroscopy to investigate the physicochemical properties of the non-aqueous RMs. Our results demonstrate that NaDEHP surfactant interacts through hydrogen bond with EG at the EG/NaDEHP interface and this interaction is responsible for destroying the bulk structure of pure solvent EG when entrapped in NaDEHP RMs. On the other hand, when DMF is incorporated inside the RMs the bulk structure of DMF is destroyed upon encapsulation by the Na-DMF interaction at the DMF/NaDEHP interface. Our results are completely different than the one observed for *n*-heptane/AOT/DMF.

Our results show how the physicochemical properties, such as micropolarity, microviscosity and hydrogen bond interaction of nonaqueous *n*-heptane/NaDEHP RMs interfaces can be dramatically changed by simply using different non-aqueous polar solvent. Thus, these results can be very useful to employ these novels RMs as nanoreactors since the dimension of the RMs are around 10 to 20 nm.

INTRODUCTION

Reverse micelles (RMs) are aggregates of surfactants formed in a non-polar solvent, in which the polar head groups of the surfactants point inward and the hydrocarbon chains point toward to the non-polar medium.¹⁻⁴ A common surfactant used to form RMs is sodium 1,4-bis-2-ethylhexylsulfosuccinate (AOT). AOT has a well-known V-shaped molecular geometry, giving rise to stable RMs without cosurfactant.¹⁻⁵ The AOT RMs has the remarkable ability to solubilize a large amount of water with values of W_0 , ($W_0 = [\text{Water}]/[\text{AOT}]$), as large as 40 to 60 depending on the surrounding non-polar medium and the temperature among others.¹⁻⁴ Besides water, some polar organic solvents, having high dielectric constants and very low solubility in hydrocarbon solvents, can also be encapsulated in reverse micelles.^{1,6} The most common polar solvents used include formamide (FA), dimethylformamide (DMF), dimethylacetamide (DMA), ethylene glycol (EG), propylene glycol (PG), and glycerol (GY).¹ The RMs in AOT/*n*-heptane systems containing these solvents are known to be spherical.¹ Also, it has been demonstrated that the size of the RMs depends on W_s ($W_s = [\text{polar solvent}]/[\text{surfactant}]$).^{7,8}

Other surfactants such as the dialkyl phosphates and their alkaline salts are of interest in extraction processes because of their complexing properties toward metal ions, which are important in hydrometallurgy, nuclear industry and biological materials.⁹ Quintana et. al.¹⁰ used the surfactant sodium bis-(2-ethylhexyl) phosphate (NaDEHP, see Scheme 1) to form aqueous RMs and they demonstrated that because of the different water–surfactant interactions the micropolarity and microviscosity of the water/NaDEHP interface, interfacial water structure, molecular probes partition and intramolecular electron transfer processes are dramatically altered in comparison to the AOT RMs systems. Surprisingly there are no reports in the literature about the study of

polar solvents, different than water, which can be encapsulated by the surfactant NaDEHP. This is a “hot topic” since it is very important in the colloidal field to explore new RMs systems, other than AOT RMs, where other polar solvent than water can be effectively encapsulated forming true RMs media in order to take all the advantages of the interface to use the RMs as nanoreactor. Bicontinuous media or nonorganized microemulsions do not do what RMs can do.

The present contribution reports the study of the different interactions between different non-aqueous polar solvents (EG, DMF) and NaDEHP polar heads in non-aqueous NaDEHP/*n*-heptane RMs, in order to gain insights on the unique RMs microenvironment created upon polar solvents encapsulation. Thus, we explore the structure of EG and DMF when encapsulated inside EG/NaDEHP/*n*-heptane and DMF/NaDEHP/*n*-heptane RMs, respectively, by using two approaches: i) non-invasive techniques such as Fourier transform infrared spectroscopy (FT-IR) and dynamic light scattering (DLS), ii) invasive technique such as absorption spectroscopy using 1-methyl-8-oxyquinolinium betaine (QB, Scheme 1) as molecular probe.

We have chosen QB as molecular probe because it is very sensitive to most of the RMs interface properties named above.^{11,12} QB is a molecular probe that has an UV-visible absorption spectrum with two major features. An absorptions band in the visible region, B₁, that is primarily sensitive to polarity, and another band peaking at shorter wavelength in the UV, B₂, which reflects the hydrogen bond donor capability of the solvent.^{11,13} The absorbance of the B₂ band is highly sensitive to the molecule's environment hence the ratio of the absorbances of B₂ to B₁ (Abs B₂/Abs B₁) in combination with the absorption bands shifts, provides an effective method to determine the properties of the microenvironment surrounding the probe.¹¹⁻¹³

We used DLS and FT-IR techniques to reveal the formation of the two reverse micellar system in *n*-heptane and also to evaluate which interaction dominates the RMs interface.

From DLS technique we substantiate the formation of EG/NaDEPH/*n*-heptane and DMF/NaDEPH/*n*-heptane instead of bicontinuous structureless microemulsions.¹ When RMs are explored, the following questions has to be answered: is the polar solvent effectively entrapped by the surfactant creating a true RMs in the organic solvent or is polar organic solvent dissolved only in the organic solvent/surfactant mixture without any molecular organization?^{1,14} Thus, DLS can be used to assess this matter because if organic polar solvents are encapsulated to form RMs interacting with the polar solvent/surfactant interface, the droplets size must increase as the W_s value increases with a linear tendency (swelling law of RMs) as it is well established for other RMs.^{1,15}

From FT-IR experiments, it is possible to monitor the changes, of the asymmetric stretching modes of the phosphate group (P=O)¹⁶⁻¹⁹ upon increase the polar solvents content and to explore the hydrogen bond interaction between EG and NaDEPH at the polar solvent/surfactant interface. The nature of the hydrogen bond in solution is of particular interest and has been investigated by diverse experimental and theoretical methods²⁰ since interface interactions play a fundamental role in the physicochemical properties of RMs.²¹

Moreover we will show here that FT-IR technique is very powerful since not only the frequency band shifts can be monitored but the band intensity as was discussed in other nonaqueous AOT RMs.¹ This will help to acquire a clear picture about how the constrained environment affects the bulk properties of the polar solvents encapsulated inside the RMs. The study of the different interactions between different non-aqueous

polar solvents (EG, DMF) and NaDEHP polar heads in non-aqueous NaDEHP/*n*-heptane RMs, in order to gain insights on the unique RMs microenvironment created upon polar solvents encapsulation is crucial to use these new RMs media as nanoreactor for nanoparticle synthesis and micellar enzymatic reactions, on which we are currently investigating.

EXPERIMENTAL SECTION

Materials

Sodium 1,4-bis (2-ethylhexyl) sulfosuccinate (AOT) from Sigma (> 99% purity), were used as received. Sodium bis-(2-ethylhexyl) phosphate (NaDEHP) was synthesized according to reference 22. Both surfactants were kept under vacuum over P₂O₅ to minimize water absorption. The absence of acidic impurities was confirmed through the 1-Methyl-8-oxyquinolinium betaine (QB) absorption bands.¹¹ QB was synthesized by a procedure reported previously.²³

n-heptane (Merck spectroscopic quality), ethylene glycol (EG) and dimethylformamide (DMF) (Sigma-Aldrich, 99% purity, HPLC grade) were used as received and ultrapure water was used throughout and prepared to a specific resistivity of > 18 MΩ cm (Labonco equipment model 90901-01).

Micellar Solutions

The stock solutions of AOT or NaDEHP in *n*-heptane were prepared by mass and volumetric dilution. To obtain optically clear solutions they were shaken in a ultrasonicating bath, and, the amount of polar solvents were added using a calibrated microsyringe. The amount of ethylene glycol (EG) and dimethylformamide (DMF) present in the system is expressed as the molar concentration ratio between polar solvent and the surfactant ($W_s = [\text{polar solvent}]/[\text{surfactant}]$). The NaDEHP

concentrations used throughout were always higher than the critical micellar concentration (cmc) which is around 10^{-3}M .¹⁰

The W_s range values studied in order to obtain optically clear solutions were $0.4 < W_s < 1$ for EG/NaDEHP/*n*-heptane and, $0.4 < W_s < 5$ for DMF/NaDEHP/*n*-heptane RMs.

Methodology

The apparent diameters (d_{app}) of the different EG/NaDEHP/*n*-heptane and DMF/NaDEHP/*n*-heptane RMs were determined by dynamic light scattering (DLS, Malvern 4700 with goniometer) with an argon-ion laser operating at 488 nm. Cleanliness of the cuvettes used for measurements was of crucial importance for obtaining reliable and reproducible data.²⁴ Quartz cuvettes were washed with ethanol, and then with doubly distilled water and dried with acetone. Prior to use, the samples were filtered three times using an Acrodisc 0.2 μm PTFE membrane (Sigma) to dust or particles presents in the original solution. Before introducing each sample to the cuvette, it was rinsed with pure *n*-heptane twice, then with the surfactant stock solution, and finally with the sample to be analyzed. Before performing measurements on a given day, the background signals from air and *n*-heptane were collected to confirm cleanliness of the cuvettes. Prior to data acquisition, the samples were equilibrated in the DLS instrument for 10 min at 25 °C. To obtain valid results from DLS measurements, knowledge of the solvent refractive index, viscosity, and well-defined conditions are required. Since we worked with dilute solutions, the refractive indices and viscosities for the RM solutions were assumed to be the same as neat *n*-heptane.²⁵ Multiple samples at each size were made, and thirty independent size measurements were made for each individual sample at the scattering angle of 90°. The instrument was calibrated before and during the course of experiments using several different size

standards. Thus, we are confident that the magnitudes obtained by DLS measurements can be statistically significant for all the systems investigated. The algorithm used was CONTIN and the DLS experiments shown that the polydispersity of the RMs were less than 5 %.

FT-IR spectra were recorded with a Nicolet IMPACT 400 FT-IR spectrometer. IR cell of the type Irtran-2 (0.5 mm of path length) from Wilmad Glass (Buena, NJ) was used. FT-IR spectra were obtained by overlaying 200 spectra at a resolution of 0.5 cm^{-1} , and the *n*-heptane spectrum was used as the background.

To introduce the molecular probe, a 0.01 M solution of QB was prepared in methanol (Sintorgan HPLC quality). The appropriate amount of this solution to obtain a concentration of 2×10^{-4} M for QB in the reverse micellar medium was transferred into a volumetric flask, and the methanol was evaporated by bubbling dry N_2 ^{11,13}; then, the surfactant RMs stock solution was added to the residue to obtain a [surfactant] = 0.1 M. The stock solution of surfactant 0.1 M and the molecular probe were agitated in a sonicating bath until the RMs was optically clear.

UV/Vis spectra were recorded using a Shimadzu 2401 spectrophotometer. The path length used in the absorption and emission experiments was 1 cm. λ_{max} was measured by taking the midpoint between the two positions of the spectrum where the absorbance is equal to $0.9 \times A_{\text{max}}$. The uncertainties in λ_{max} were about 0.1 nm.

RESULTS AND DISCUSSION

*Non-aqueous NaDEHP/*n*-heptane RMs explored by DLS.*

In order to confirm the presence of nonaqueous NaDEHP RMs, DLS measurements were carried out for two systems: EG/NaDEHP/*n*-heptane and DMF/NaDEHP/*n*-heptane, at different W_s and at [NaDEHP] = 0.1 M. The droplets sizes values obtained in both systems are reported in Figure 1 A and B. It is shown that

different tendency is obtained depending on the polar solvent entrapped. Additionally, the range of W_s obtained giving a clear solution is also different between RMs.

Figure 1 A demonstrates an increase in the droplets size values when the EG content increases. For example, the apparent diameter (d_{app}) value for the RMs at $W_s = 0.4$ is 9.0 nm and this value increases up to 22.5 nm at $W_s = 1$. The tendency observed, indicates that EG molecules are effectively entrapped in the organized system and that RMs are not interacting among each other.²⁶ It is important to remark that the d_{app} values obtained for NaDEHP/*n*-heptane RMs are larger than the corresponding values reported for the EG/AOT/*n*-heptane RMs.¹⁵ For example, the d_{app} value reported¹⁵ in the system EG/AOT/*n*-heptane at $W_s = 0$ is 2.2 nm and increases up to 5.4 nm at $W_s = 1$. To interpret these results it is important to consider that the RMs droplet sizes depend, among many other variables, on interactions between the surfactant and the polar solvent. It is known that when water is encapsulated in AOT/*n*-heptane RMs, the hydrogen-bond interaction of water molecules with the AOT polar head groups increases the surfactant's head group cross-section area, a , thus decreases the surfactant packing parameter P_c ($P_c = v/al_c$, where v and l_c are the volume and the length of hydrophobic chain, respectively, and a the cross-section area of polar head group of the surfactant) and, increases the RMs droplet size.^{27,28}

As EG is a kind of solvent similar to water in the way that it can interact through hydrogen bond with the phosphate group of NaDEHP; our results indicate that when EG molecules are encapsulated by NaDEHP RMs, their interact ion with the surfactant molecules through hydrogen bond changes the a value, thereby increasing the RMs droplet sizes. Furthermore, the droplets sizes of the RMs formed in the system EG/NaDEHP/*n*-heptane, is approximately 4 times larger than those formed by EG/AOT/*n*-heptane.²⁶ It must be noted that the plot in Figure 1 A shows a deviation

from linearity as the W_s value increases, which suggests that the EG/NaDEHP/*n*-heptane RMs may be ellipsoidal rather than spherical micelles.

The droplets size values obtained in DMF/NaDEHP/*n*-heptane RMs are shown in Figure 1 B. It shows that, the d_{app} values decreases to a minimum at $W_s \sim 3$ and then start to increase gradually until the maximum W_s ($W_s = 5$), which could be reached form a single phase. Figure 1 B demonstrates a different behavior in comparison with that obtained in the system DMF/AOT/*n*-heptane²⁹, where, the d_{app} values of RMs increases slightly with the DMF content. However, Figure 1B shows the RMs behavior is similar to that of the water/NaDEHP/*n*-heptane^{30,31} and water/NaDEHP/benzene^{32,33} where a minimum in the d_{app} value appears around $W_0 \sim 3$. Deviation from the linearity could be due to several factors, the most relevant might be: droplet–droplet interaction and/or other RMs shape.^{15,26,30,34} Shelly et. al.^{32,33} studied several properties of the system water/NaDEHP/benzene and they suggested that below the "critical water content" ($W_0 \sim 3$) the micelles are large rod-shaped dipolar crystallites with the same structure as the constituent rods of the hexagonal liquid crystalline solid state of NaDEHP. At $W_0 > 3$ they have shown that the large micelles successively dissolve and become spherical RMs which sizes growth with the W_0 value.

Similarly, the results obtained in the DMF/NaDEHP/*n*-heptane can be interpreted in the following way. When DMF is encapsulated inside NaDEHP/*n*-heptane RMs, micelle shape would incurred a change from the ellipsoidal ($W_s \leq 3$) to spherical ($W_s > 3$), similar to results found by Shelly et. al.^{32,33} for aqueous NaDEHP RMs. Upon $W_s > 3$, the NaDEHP molecules on the RM/*n*-heptane interface, are totally solvated by DMF and we observed how the d_{app} values of RMs increases with DMF content, indicating that DMF molecules are effectively entrapped inside the organized system and that RMs are not interacting with droplets. It is also necessary to highlight that the

d_{app} values obtained in DMF/NaDEHP/*n*-heptane are larger than the obtained for DMF/AOT/*n*-heptane^{15,26} RMs. For example, the d_{app} value found in the system DMF/AOT/*n*-heptane at $W_s = 1$ is 2.5 nm in comparison with DMF/NaDEHP/*n*-heptane RMs where is 15.7 nm at the same W_s . Another interesting result is that the RMs sizes grow faster than the sizes of AOT RMs while increasing W_s .¹⁵ It is known that DMF do not have hydrogen atom to form hydrogen bond interactions and when these molecules are encapsulated in AOT/*n*-heptane RMs, DMF neither interact with the C=O nor with the SO_3^- groups but their weakly bulk associated structure is broken because of their coordination with Na^+ .²⁶ We propose that in DMF/NaDEHP/*n*-heptane the free electron pairs of the carbonyl and nitrogen groups of DMF sequestered by RMs can interact with the NaDEHP sodium counterions. However, in contrast to AOT, it seems that DMF could form part of the interface affecting the surfactant packing parameter P_c and hence the RMs sizes and shape. What is important to highlight is that the behavior of the encapsulated DMF is similar to the one observed in aqueous NaDEHP RMs, despite the very different structure of the polar solvent.

In order to evaluate differences in the unique NaDEHP RMs interfacial physicochemical properties such as micropolarity and hydrogen bond interaction, we have studied the solvatochromic behavior of QB in EG/NaDEHP/*n*-heptane and DMF/NaDEHP/*n*-heptane RMs by means of absorption spectroscopy, at different W_s . It must be noted that the molecular probe resides mainly at the DMF/NaDEHP and EG/NaDEHP interfaces in the RMs since QB is not soluble in the organic phase.¹ Thus, QB can monitor the physicochemical changes at these RMs interfaces.

QB in EG/NaDEHP/*n*-heptane and DMF/NaDEHP/*n*-heptane RMs.

Table 1 demonstrates the values of λ_{\max} B₁ and B₂ for QB in pure EG and DMF, respectively, as well as the Abs B₂/Abs B₁ ratio taken at the λ_{\max} of each bands.

Analysis of QB λ_{\max} B₁ and B₂ values shows that both bands undergo hypsochromic shifts (shift to a shorter wavelength in the absorption spectrum) when the polarity/polarizability (π^*) and the hydrogen bond donor capability (α) of the medium increases. Also the ratio AbsB₂/AbsB₁, in combination with the absorption bands shifts, provide an effective method to determine the properties of the microenvironment surrounding the probe as it was described before.^{12,13} Here, we highlight that the ratio values obtained in DMF is three times larger than EG, confirming the absence of hydrogen bond interaction.^{1,12}

Figure 2 shows the QB absorption spectra with varying W_s at [QB] = 2×10^{-4} M and [NaDEHP] = 0.1 M in EG/NaDEHP/*n*-heptane RMs. Figures 3 A and B summarize the λ_{\max} B₁ and the AbsB₂/AbsB₁ ratio values for QB in EG/NaDEHP/*n*-heptane RMs. Also, data from EG/AOT/*n*-heptane RMs are shown for comparison. As shown in Figures 3 A, there are hypsochromic shifts of the B₁ bands with EG content increase, indicating that QB is sensing a more polar environment. As expected, at low W_s the probe located at interface of NaDEHP/*n*-heptane RMs, QB is sensing the interaction between EG molecules and NADEHP at the interface. Figure 2 shows how the absorbance of the B₁ band remains practically constant while the absorbance of the B₂ band decreases as the W_s increases, indicating that the molecule is sensing the hydrogen bond interaction at the micellar interface, as observed in Figure 3 B.

Figure 3 A also shows differences between AOT and NaDEHP RMs interfaces. For EG/AOT/*n*-heptane system, the hypsochromic shift observed in the λ_{\max} B₁ is more significant and reaches similar values to the λ_{\max} B₁ obtained in pure EG (see Table 1), at high W_s . This behavior would indicate that QB is anchored at the interface at low W_s ;

at high W_s values QB is dissolved in the polar core of the micelles, where the polarity and structure of EG is similar to that found in pure solvent. Similar tendencies was found in previous work¹⁰ for water encapsulated in water/NaDEHP/*n*-heptane RMs where water molecules formed hydrogen bond interactions with QB anchored at the interface at low W_0 , at high water content QB is expelled to the water pool where the water structure is similar to the pure solvent. On the other hand, in EG/NaDEHP/*n*-heptane RMs, the shift observed in $\lambda_{\max} B_1$ never reaches the value observed in the pure solvent. This suggests that when QB molecules are anchored to the EG/NaDEHP interface, their interactions through hydrogen bond with EG are stronger than those when AOT is the surfactant. In addition, this interaction is responsible for destroying the bulk EG structure. Thus, the stronger EG-NaDEHP interaction in comparison with EG-AOT interaction would be responsible for the large droplet sizes found in EG/NaDEHP/*n*-heptane RMs by DLS technique.

It is interesting to compare the $AbsB_2/AbsB_1$ ratio values for AOT and NaDEHP RMs at different W_s . Figure 3 B shows that there is a significant diminishing in the $AbsB_2/AbsB_1$ values with the increases of the EG content in both systems (NaDEHP and AOT) which is consistent with the greater hydrogen bond donor ability of the medium upon RMs formation. At the W_s maximum value in EG/AOT/*n*-heptane, QB detects a $AbsB_2/AbsB_1$ value close to that found in pure solvent. On the other hand, for EG/NaDEHP/*n*-heptane RMs, the ratio value is quite far from that found in pure solvent. This result confirms what discussed above, apparently, EG forms stronger hydrogen bond interaction with the polar head of NaDEHP than with AOT. Consequently, the structure of EG inside EG/NaDEHP/*n*-heptane RMs is different from those found in the pure solvent and in AOT RMs.

However, the situation is quite different when DMF is encapsulated inside NaDEHP RMs. Figure 4 shows the QB absorption spectra with varying W_s at $[QB] = 2 \times 10^{-4}$ M and $[NaDEHP] = 0.1$ M for DMF/NaDEHP/*n*-heptane RMs. Figures 5 A and B summarize the λ_{max} B_1 and the $Abs B_2/Abs B_1$ ratio values for QB in DMF/NaDEHP/*n*-heptane and in DMF/AOT/*n*-heptane varying W_s at 0.1 M concentration of the surfactants, respectively.

Figure 4 shows that in NaDEHP RMs the B_1 and B_2 bands present a bathochromic shift (shift to a longer wavelength in the absorption spectrum) when DMF content increases. This shifting observed was not expected since when W_s increases the polarity of the DMF/NaDEHP and NaDEHP/*n*-heptane interface should also increase, and both bands should show hypsochromic shift.¹¹ Furthermore, the intensity of the B_2 band increases markedly with the increase of the DMF content and, this band should remain constant if the DMF molecules have no-interaction with NaDEHP through hydrogen bonding.

Figure 5 A, interestingly, shows that the QB behavior in NaDEHP RMs is completely different than what found in AOT RMs.¹² The system DMF/NaDEHP/*n*-heptane shows a bathochromic shift in the λ_{max} B_1 when DMF content increases, indicating that QB senses a reduction in the interfacial polarity as the DMF content increases. This phenomenon is clearly different from that found for AOT RMs, where the shift is hypsochromic with increasing W_s , showing an increase in the interfacial polarity. Moreover, QB in DMF/AOT/*n*-heptane RMs senses a more polar microenvironment inside the RMs, even larger than the pure DMF. In DMF/NaDEHP/*n*-heptane RMs as the DMF content increases, the behavior was expected, the polarity sensed by QB decreases to reach the value of the pure solvent but never reaches its value.¹² Also, Figure 5 A shows that, in DMF/NaDEHP/*n*-heptane

RMs, a break appears at $W_s \sim 3$, indicating that QB also detects the change of the RMs shape suggested in Section 1 using DLS technique.

Figure 5 B, shows the $AbsB_2/AbsB_1$ ratio for DMF/AOT/*n*-heptane RMs. The absorbance ratio is constant in the whole W_s range studied because DMF cannot form hydrogen bond interactions. On the other hand, different behavior was observed for QB in DMF/NaDEHP/*n*-heptane RMs, where the $AbsB_2/AbsB_1$ ratio value increases with the DMF content. Also, a break is observed around $W_s = 3$, which would evidence again the possible change in the shape of the system DMF /NaDEHP/ *n*-heptane.

In others words, these results obtained for both RMs systems suggest that DMF interacts in different manner with different surfactant polar heads groups.

EG/NaDEHP/*n*-heptane and DMF/NaDEHP/*n*-heptane RMs explored by FT-IR spectroscopy

FT-IR measurements were carried out for the two RMs systems studied: EG/NaDEHP/*n*-heptane and DMF/NaDEHP/*n*-heptane, at different W_s and at $[NaDEHP] = 0.01$ M. This different concentration was chosen to obtain non-saturated FTIR spectra and it was above the cmc value.¹⁰ Here, we follow the changes in the asymmetric stretching band of the phosphate group (P=O) of NaDEHP by varying the EG and DMF content. From the analysis of the changes obtained from the IR spectra, the structural information about the NaDEHP RMs interface could be evaluated, when EG or DMF are inside the polar core. Scheme 2 shows the structure of the phosphate group of bis(2-ethylhexyl) phosphoric acid (HDEHP) and the NaDEHP surfactant.

Note that the P=O bond is no longer present in NaDEHP since the group $[O-P-O]^-$ is formed due to the electron-cloud delocalization.³⁵ Frequency for P=O stretching (1252 cm^{-1}) in HDEHP is reasonably displaced in NaDEHP by two frequencies, i.e.,

1229 cm^{-1} for the asymmetrical and 1120-1050 cm^{-1} for the symmetrical, which is overlapped with the strong absorption band around 1032 cm^{-1} for the [P-O-C] stretching and for this reason we have only investigated the shifts in the asymmetric stretching band.³⁵

Figure 6 A and B show the FT-IR spectra and the shift corresponding to the asymmetric stretching mode of the P=O group band of EG/NaDEHP/*n*-heptane RMs varying W_s , respectively. Figure 6 shows that, upon the addition of EG to the NaDEHP/*n*-heptane RMs, a shift in the asymmetric P=O stretching band to lower frequencies (from 1241 cm^{-1} to 1203 cm^{-1}) was observed when the W_s values increased from 0 to 1.5. Furthermore, Figure 6A demonstrates changes in the intensity of the bands when the EG content increases. Li et. al. studied the FT-IR spectra of the system water/NaDEHP/*n*-heptane¹⁶⁻¹⁹ and they demonstrated that the water inside RMs can interact through hydrogen bond with the phosphate group of NaDEHP and that the water, at the same time, can interact with the Na^+ counterion by the ion-dipole interaction. The hydrogen bond interaction weakens the P=O bond with increasing the water content reflecting in the decrease in the frequency values of the asymmetric phosphate stretching band. As EG is a solvent similar to water in the way that it can interact through hydrogen bond with the phosphate group of NaDEHP RMs (see Scheme 3 for schematic representation); our results indicate that this interaction occurs and consequently weakens the P=O bond.

Figure 7 A and B show the typical FT-IR spectra and the shift corresponding to the asymmetric stretching mode of the phosphate group band of DMF/NaDEHP/*n*-heptane RMs at different W_s value, respectively. We observed that in the DMF/NaDEHP/*n*-heptane RMs the asymmetric stretching band of the P = O bond is centered at 1241 cm^{-1} when $W_s = 0$ with a slight shoulder at 1260 cm^{-1} . This shoulder

begins to growth when the DMF content increases. It is known³⁶ that N-C stretching of the amide is observed in a frequency range around 1260 cm^{-1} , so this new band could be assigned to DMF encapsulated inside the DMF/NaDEHP/*n*-heptane RMs, which appears in a region of the spectrum near the phosphate group band of the NaDEHP surfactant. Note that the frequency of the band remains constant ($\nu\sim 1241\text{ cm}^{-1}$) with increasing W_s , which clearly indicates that the DMF molecules are not interacting with the phosphate group. Furthermore, it is known that DMF does not form hydrogen bond, however, DMF has high affinity to solvate cations.³⁷⁻³⁹ Other studies⁴⁰⁻⁴³ performed by techniques such as Raman, FT-IR and NMR showed that when different metal ions are dissolved in DMF, and induce a specific structuration in DMF, showing a preferential solvation. These facts help explain the results since the DMF molecules inside of RMs would interact with the Na^+ counterion through free electrons of the carbonyl and nitrogen groups, without interacting with the phosphate group of NaDEHP surfactant (Scheme 3).

CONCLUSIONS

In this work, we use the dynamic light scattering (DLS) technique to confirm the formation of two novel nonaqueous NaDEHP/*n*-heptane RMs using EG and DMF as polar component.

Using the solvatochromism behavior of the molecular probe, QB, we demonstrate that NaDEHP surfactant interacts through hydrogen bond with EG at the EG/NaDEHP interface and this interaction is responsible for the disruption of the structure of pure solvent EG when entrapped in NaDEHP RMs. On the other hand, when DMF is incorporated into the NaDEHP RMs, the RMs shape changes with the DMF content, from ellipsoidal or rod-like to spherical RMs in similar manner to what it

was observed in water/NaDEHP/*n*-heptane system. This is quite odd considering the completely pure solvent structure of water in comparison with DMF. We suggest that DMF bulk structure is destroyed upon encapsulation for the Na⁺-DMF interaction at the interface. Thus, DMF forms part of the RMs interface changing the packing parameter P_c . Results that are completely different from the phenomena observed for DMF/AOT/*n*-heptane.

Furthermore, FT-IR has been used to explore the asymmetric P=O stretching modes of NaDEHP in these RMs. We found that EG interact with the surfactant molecules through hydrogen bond and consequently weakens the P=O bond, which is reflected in a decrease in the frequency values of asymmetric stretching band of phosphate group. When DMF is encapsulated inside the RMs, DMF molecules do not interact with the phosphate group because of its high capacity to solvate Na⁺ inside RMs. We suggest that DMF can complex with the Na⁺ ions through their carbonyl and amide groups.

In summary, the work shows how the micropolarity, hydrogen bond interaction and polar solvent structure for the novel NaDEHP/*n*-heptane RMs interfaces can be dramatically changed simply using different non-aqueous polar solvent. Since EG and DMF are very dissimilar in their approaches to interact with RMs interface, these phenomena could have interesting consequences in different reaction to nanoscale.¹ Thus, these results can be very useful to employ these novels RMs as nanoreactors.

ACKNOWLEDGEMENTS

We gratefully acknowledge the financial support for this work by the Consejo Nacional de Investigaciones Científicas y Técnicas (CONICET), Agencia Córdoba Ciencia, Agencia Nacional de Promoción Científica y Técnica and Secretaría de Ciencia y Técnica de la Universidad Nacional de Río Cuarto. F.M., J.J.S., R.D.F and N.M.C.,

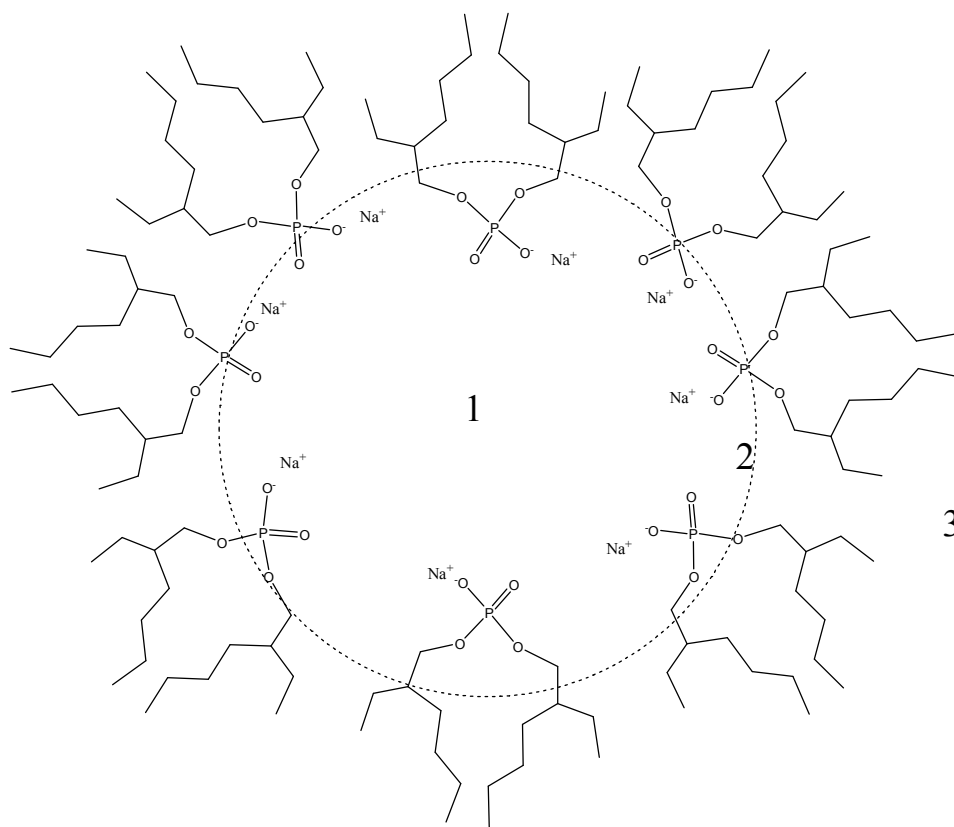
hold a research position at CONICET. S.S.Q. thanks CONICET for a research fellowship. We also want to thank referee 4 for his/her careful and thorough review of this manuscript.

REFERENCES

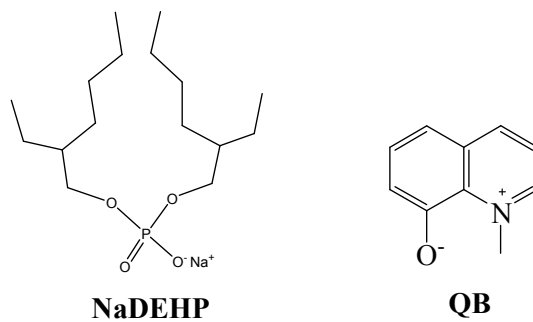
- 1 N. M. Correa, J. J. Silber, R. E. Riter, N. E. Levinger, *Chem. Rev.*, 2012, **112**, 4569.
- 2 J. J. Silber, M. A. Biasutti, E. Abuin, E. Lissi, *Adv. Colloid Interface Sci.*, 1999, **82**, 189.
- 3 T. K. De, A. Maitra, *Adv. Colloid Interface Sci.*, 1995, **59**, 95.
- 4 S. P. Moulik, B. K. Paul, *Adv. Colloid Interface Sci.*, 1998, **78**, 99.
- 5 M. A. Biasutti, E. B. Abuin, J. J. Silber, N. M. Correa, E. A. Lissi, *Adv. Colloid Interface Sci.*, 2008, **136**, 1.
- 6 A. Martino, E. W. Kaler, *J. Phys. Chem.*, 1990, **94**, 1627.
- 7 P. D. I. Fletcher, M. F. Galal, B. H. Robinson, *J. Chem. Soc., Faraday Trans. 1*, 1984, **80**, 3307.
- 8 E. R. Riter, J. R. Kimmel, E. P. Undiks, N. E. Levinger, *J. Phys. Chem. B*, 1997, **101**, 8292.
- 9 L.C. Dong, S.J. Huang, Q. Luo, X.H. Zhou, S.S. Zheng, *Biochem. Eng. J.*, 2009, **46**, 210.
- 10 S. S. Quintana, R. D. Falcone, J. J. Silber, N. M. Correa, *ChemPhysChem*, 2012, **13**, 115.
- 11 N. M. Correa, M. A. Biasutti, J.J. Silber, *J. Colloid. Interface. Sci.*, 1995, **172**, 71.
- 12 R. D. Falcone, N. M. Correa, M. A. Biasutti, J. J. Silber, *Langmuir* 2000, **16**, 3070.
- 13 N. M. Correa, M. A. Biasutti, J.J. Silber, *J. Colloid Interface Sci.*, 1996, **184**, 570.

- 14 A. M. Durantini, R. D. Falcone, J. J. Silber, N. M. Correa, *J. Phys Chem B*, 2013, **117**, 3818.
- 15 R. D. Falcone, J. J. Silber, N. M. Correa, *Phys. Chem. Chem. Phys*, 2009, **11**, 11096.
- 16 Q. Li, S. Weng, J. Wu, H. Zhou, *J. Phys. Chem B*, 1998, **102**, 3168.
- 17 N. Zhou, Q. Li, J. Wu, J. Chen, S. Weng, G. Xu, *Langmuir*, 2001, **17**, 4505.
- 18 Q. Li, J. Wu, N. Zhou, *J. Colloid Interface Sci*, 2000, **229**, 298.
- 19 Q. Li, T. Li, J. Wu, *J. Phys. Chem B*, 2000, **104**, 9011.
- 20 G. J. Zhao, k. L. Han, *J. Phys. Chem A*, 2007, **111**, 2469.
- 21 G. J. Zhao, k. L. Han. *Acc. Chem. Res.*, 2012, **45(3)**, 404.
- 22 A. Ruggirello, V.T. Liveri, *J. Colloid Interface Sci*, 2003, **258**, 123.
- 23 M. Ueda, Z. A. Schelly, *Langmuir*, 1989, **5**, 1005.
- 24 M. A. Sedgwick, A. M. Trujillo, N. Hendricks, N. E. Levinger, D. C. Crans, *Langmuir*, 2011, **27**, 948.
- 25 J. P. Blitz, J. L. Fulton, R. D. Smith, *J. Phys. Chem*, 1988, **92**, 2707.
- 26 A. M. Durantini, R. D. Falcone, J. J Silber, *J. Phys. Chem. B*, 2011, **115**, 5894.
- 27 D. F. Evans, B. W. Ninham, *J. Phys. Chem*, 1986, **90**, 226.
- 28 Q. Li, T. Li, J. Wu, *J. Colloid Interface Sci*, 2001, **239**, 522.
- 29 A. M. Durantini, R. D. Falcone, J. J Silber, *J. Phys. Chem. B*, 2011, **115**, 5894.
- 30 Z. J. Yu, R. D. Neuman, *J. Am. Chem. Soc*, 1994, **116**, 4075.
- 31 Z. J. Yu, R. D. Neuman, *Langmuir*, 1995, **11**, 1081.
- 32 K. I. Feng, Z. A. Schelly, *J. Phys. Chem*, 1995, **99**, 17207.
- 33 K. I. Feng, Z. A. Schelly, *J. Phys. Chem*, 1996, **99**, 17212.
- 34 P. L. Luisi, M. Giomini, M. P. Pileni B. H. Robinson, *Biochem. Biophys. Acta*, 1988, **947**, 209.

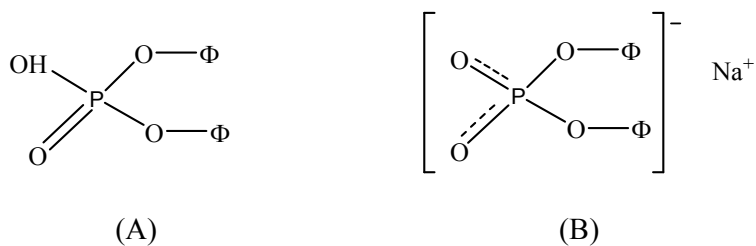
- 35 J. G. Wu, N. Shi, H. C. Gao, *Sci. Sinica, Ser. B*, 1984, **27**, 249.
- 36 E. Pretsch, P. Buhlmann, C. Affolter, *Structure Determination of Organic Compounds*, Tables of Spectral Data, Ed. Springer-Verlag Berlin Heidelberg, 2000, 296.
- 37 Y. P. Puhovski, L. P. Safanova, B. M. Rode, *J. Mol. Liquid*, 2003, **103**, 15.
- 38 J. Barthel, R. Buchner, B. Wurm, *J. Mol. Liquid*, 2002, **98**, 51.
- 39 C. M. Criss, E. Luksha, *J. Phys. Chem*, 1968, **72**, 2966.
- 40 M. S. Akhter, S. M. Alawi, *Colloids Surf. A: Physicochem. Eng. Aspects*, 2003, **219**, 281.
- 41 E. Hirota, R. Sugisaki, C. J. Nielsen, G. O. Sorensen, *J. Mol. Spectrosc*, 1974, **49**, 251.
- 42 D. J. Gardiner, J. A. Lees, B. P. Straughan, *J. Mol. Struct*, 1979, **53**, 15.
- 43 J. A. Lees, B. P. Straughan, D. J. Gardiner, *J. Mol. Struct*, 1981, **71**, 61.



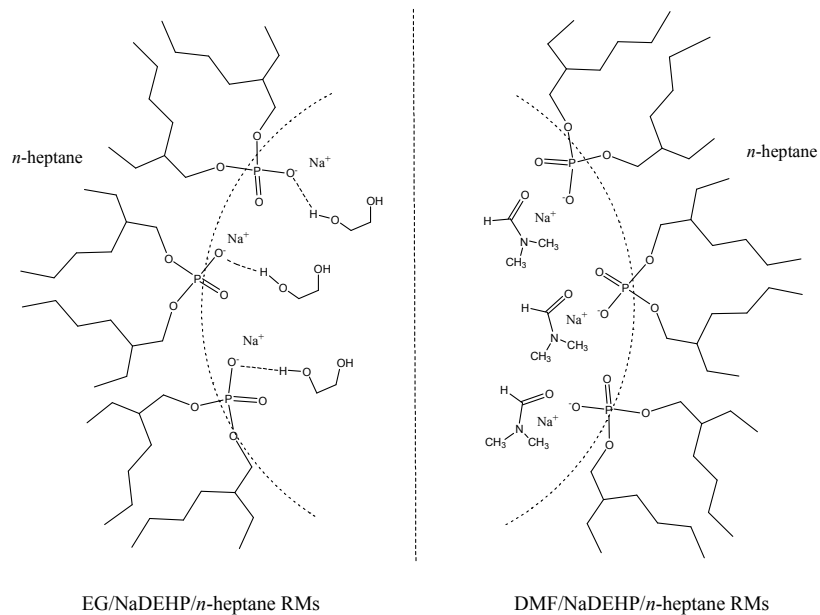
NaDEHP/*n*-heptane RMs



Scheme 1. Schematic representation of NaDEHP/*n*-heptane RMs and, molecular structures of the surfactant NaDEHP and the molecular probe QB. (1) Polar solvent, (2) micelles interface, (3) non-polar organic solvent.



Scheme 2. Structure of the bond phosphate group (P = O) in (A) HDEHP and (B) NaDEHP. The symbol Φ corresponds to 2-ethyl-hexyl groups in both cases.



Scheme 3. Schematic representation of the polar molecules (EG and DMF) interaction at the interface in nonaqueous *n*-heptane/NaDEHP RMs.

Table 1. The maxima absorption wavelength of B₁ and B₂ and, the absorbance ratio (Abs B₂ / Abs B₁) values of QB in different polar solvents. [QB] = 2x10⁻⁴ M.

Solvent	π^{*a}	α^a	$\lambda_{\max}B_1/\text{nm}$	$\lambda_{\max}B_2/\text{nm}$	AbsB ₂ / AbsB ₁
EG	0.92	0.90	464	355	1.16
DMF	0.88	0.00	546	381	3.07

^a Value from Ref 12

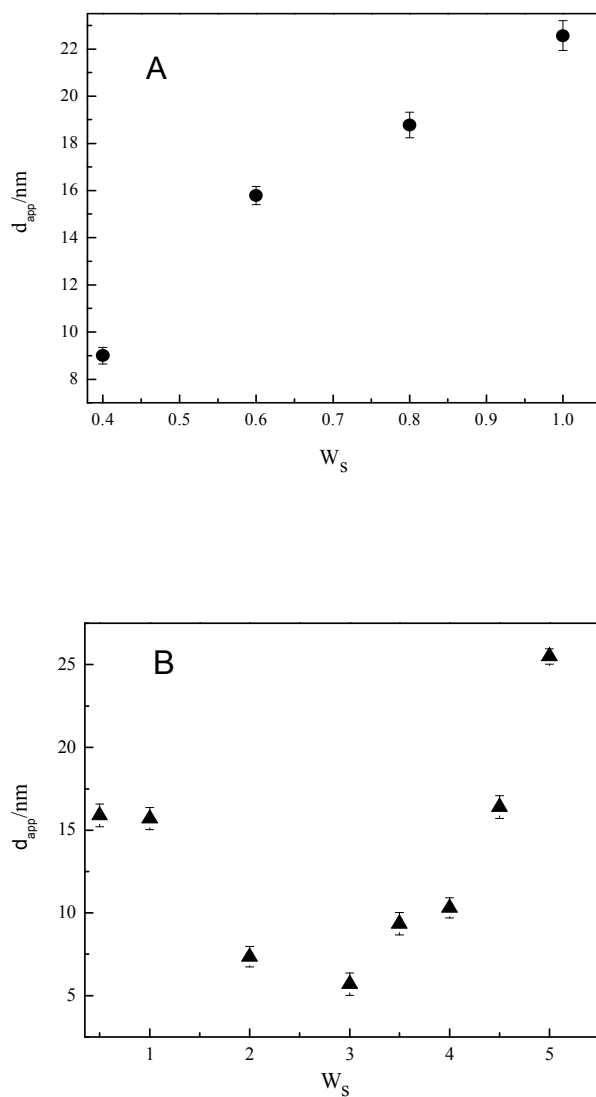


Figure 1. A) The apparent diameter (d_{app}) values of the EG/NaDEHP/*n*-heptane obtained at 25 °C varying W_s . [NaDEHP] = 0.1 M. B) The d_{app} values of the DMF /NaDEHP/*n*-heptane obtained at 25 °C varying W_s . [NaDEHP] = 0.1 M.

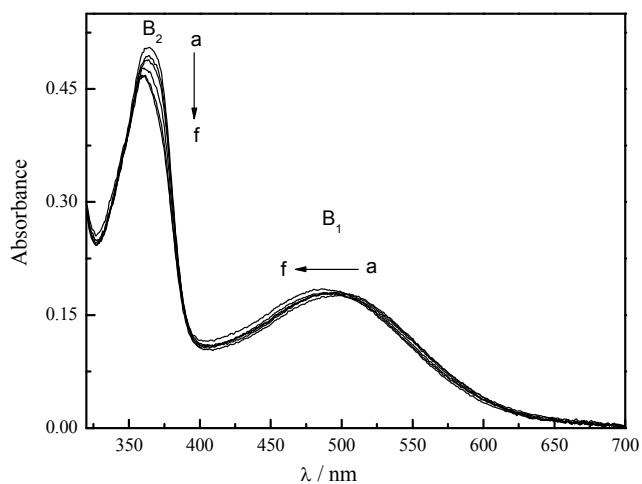


Figure 2. QB absorption spectra in EG/NaDEHP/*n*-heptane RMs as a function of W_s . W_s : (a) 0.4, (b) 0.5, (c) 0.6, (d) 0.8, (e) 1, (f) 1.2. $[QB] = 2 \times 10^{-4}$ M. $[NaDEHP] = 0.1$ M.

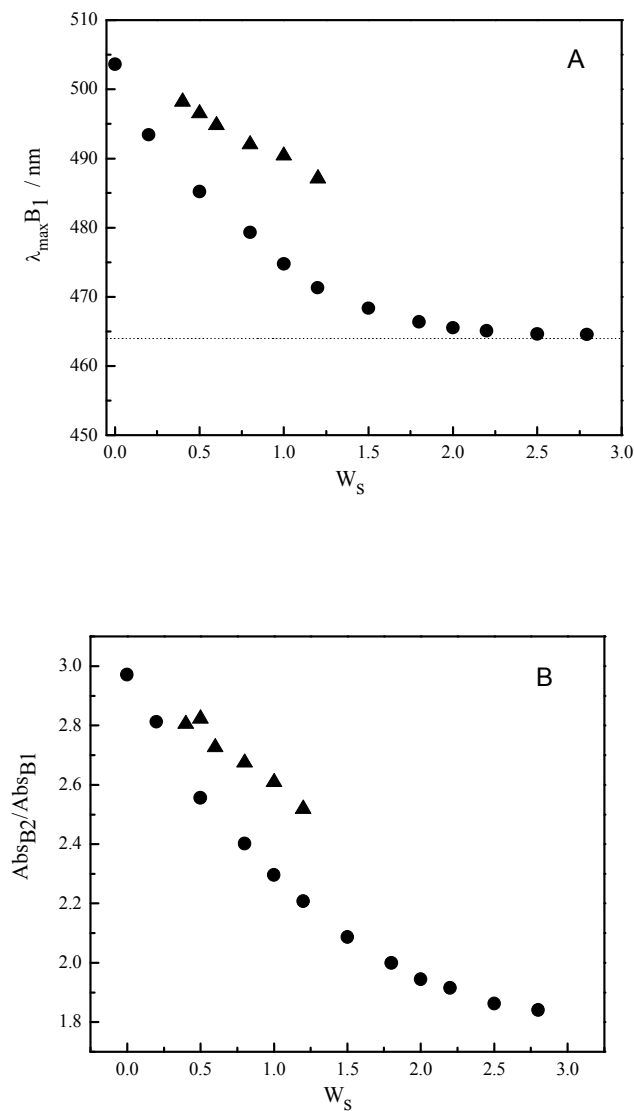


Figure 3. A) Variation of B₁ band ($\lambda_{\max} B_1$) in (▲)EG/NaDEHP/*n*-heptane and (●)EG/AOT/*n*-heptane as a function of W_s . [QB] = 2×10^{-4} M. [Surfactant] = 0.1 M. The $\lambda_{\max} B_1$ value (dot line) corresponding to neat EG is included for comparison. B) Variation of $\text{Abs}B_2 / \text{Abs}B_1$ in (▲) EG/NaDEHP/*n*-heptane and (●) EG/AOT/*n*-heptane as a function of W_s . [QB] = 2×10^{-4} M. [Surfactant] = 0.1M.

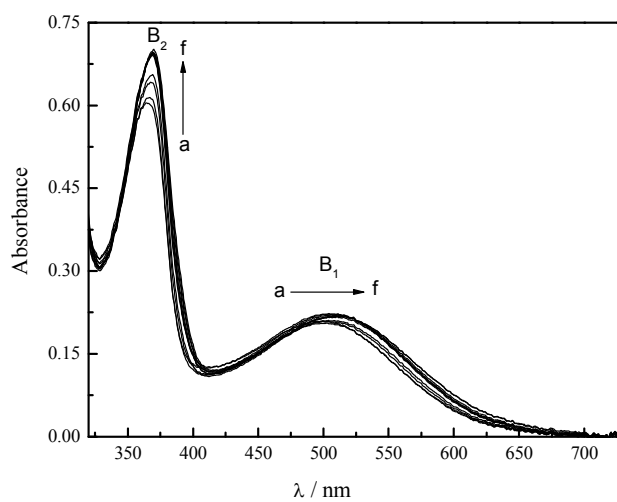


Figure 4. QB absorption spectra in DMF/NaDEHP/*n*-heptane RMs as a function of W_s .

W_s : (a) 0.5, (b) 1, (c) 2, (d) 3, (e) 4, (f) 5.5. $[QB] = 2 \times 10^{-4}$ M. $[NaDEHP] = 0.1$ M.

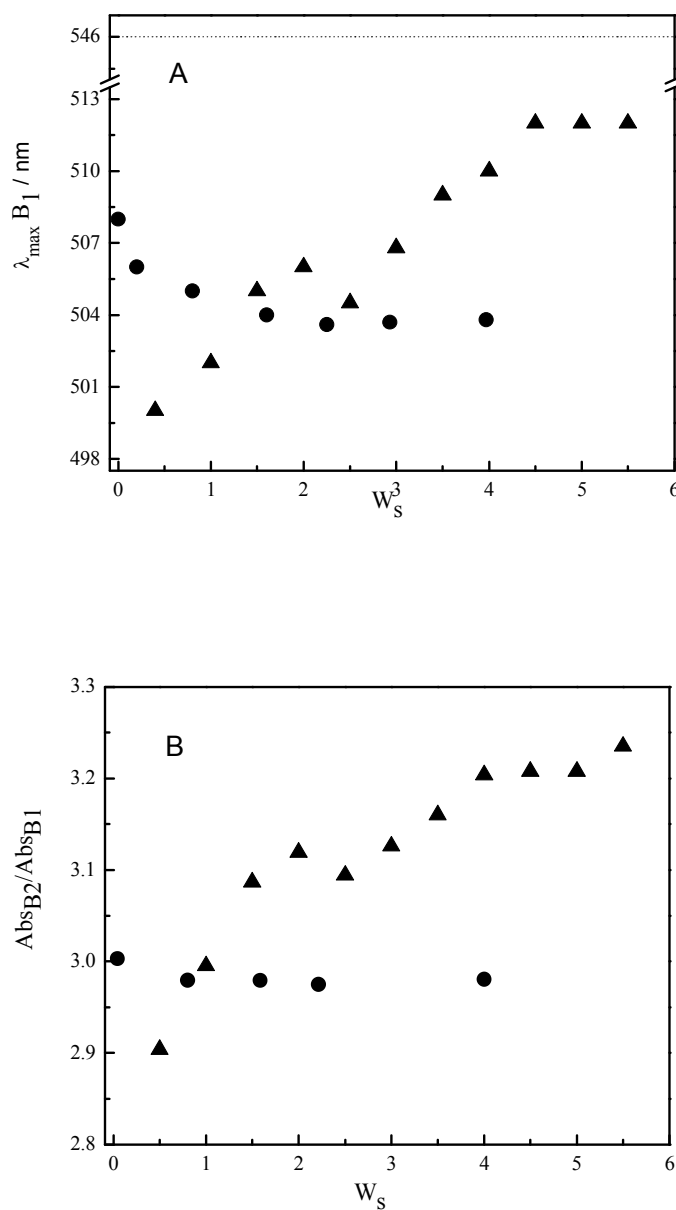


Figure 5. A) Variation of B₁ band ($\lambda_{\max} B_1$) in (▲) DMF/NaDEHP/*n*-heptane and (●) DMF/AOT/*n*-heptane as a function of W_s . [QB] = 2×10^{-4} M. [Surfactant] = 0.1 M. The $\lambda_{\max} B_1$ value (dot line) corresponding to neat DMF is included for comparison. B) Variation of $\text{Abs}_{B_2} / \text{Abs}_{B_1}$ in (▲) DMF/NaDEHP/*n*-heptane and (●) DMF/AOT/*n*-heptane as a function of W_s . [QB] = 2×10^{-4} M. [Surfactant] = 0.1 M.

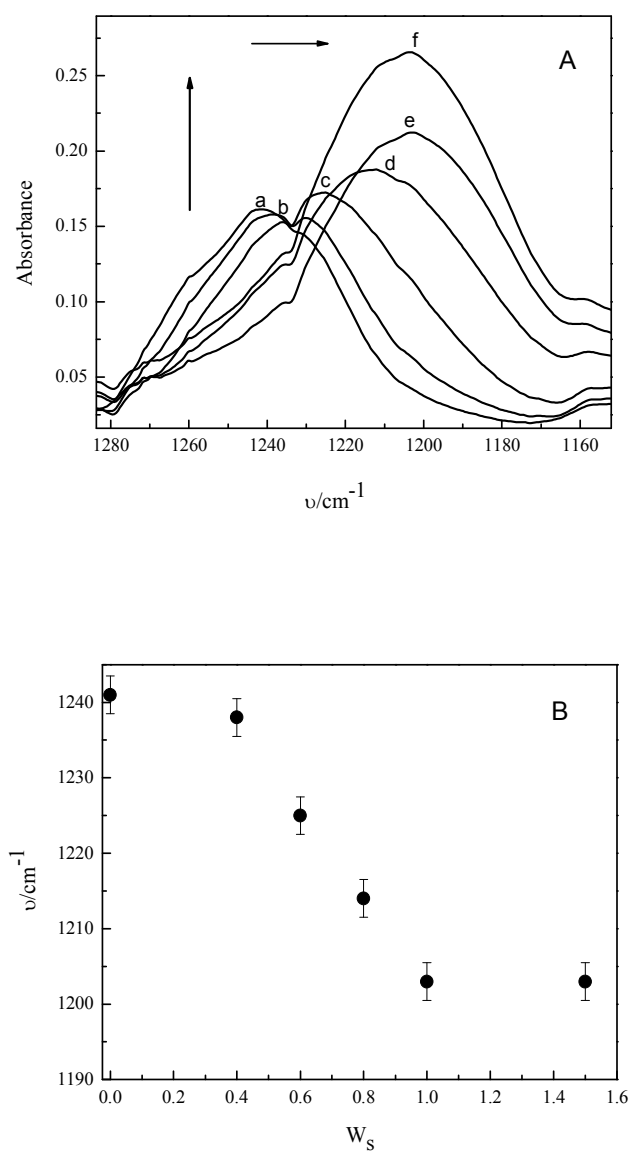


Figure 6. A) FT-IR spectra of EG/NaDEHP/*n*-heptane RMs at different W_s values, in the region of 1160-1280 cm^{-1} (NaDEHP's ν_{PO}). W_s : a) 0, b) 0.4, c) 0.6, d) 0.8, e) 1.0, f) 1.5. B) Shift of the NaDEHP's asymmetric phosphate stretching frequency (ν_{PO}) upon increases W_s in EG/NaDEHP/*n*-heptane RMs. W_s : a) 0, b) 0.4, c) 0.6, d) 0.8, e) 1.0, f) 1.5.

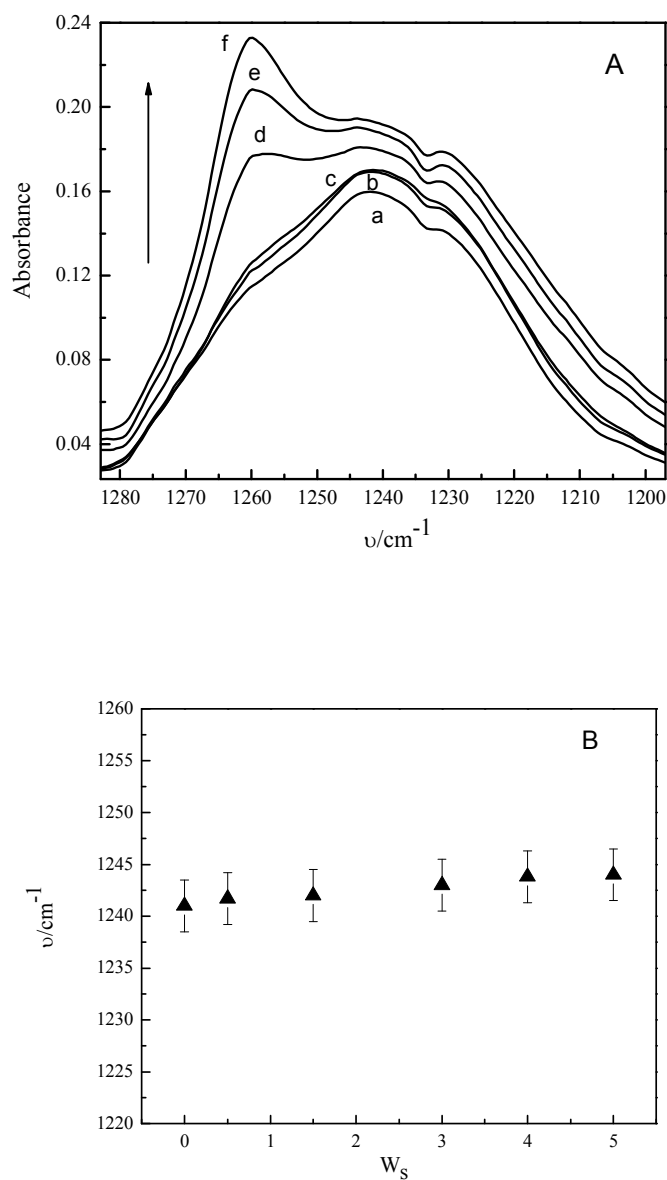


Figure 7. A) FT-IR spectra of DMF/NaDEHP/*n*-heptane RMs at different W_s values, in the region of 1200-1280 cm^{-1} (NaDEHP's ν_{PO}). W_s : a) 0, b) 0.5, c) 1.5, d) 3, e) 4, f) 5.

B) Shift of the NaDEHP's asymmetric phosphate stretching frequency (ν_{PO}) upon increases W_s in DMF/NaDEHP/*n*-heptane RMs. W_s : a) 0, b) 0.5, c) 1.5, d) 3, e) 4, f) 5.